SECOND INTERNATIONAL SYMPOSIUM ON INNOVATIVE NUMERICAL ANALYSIS IN APPLIED ENGINEERING SCIENCE

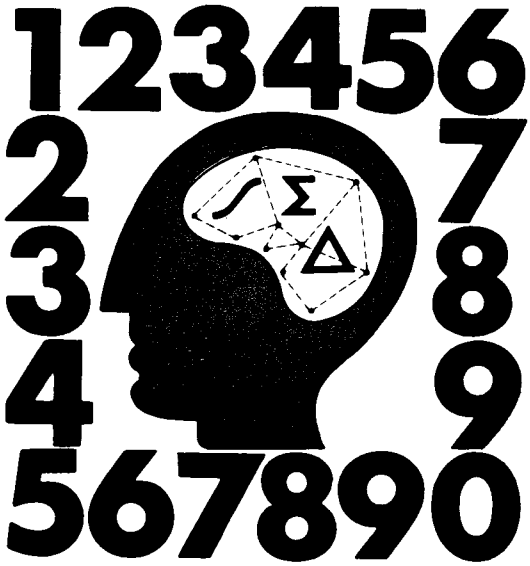

DEUXIEME COLLOQUE INTERNATIONAL SUR LES DEVELOPPEMENTS NOUVEAUX DANS LES METHODES NUMERIQUES DE L'INGENIEUR

ECOLE POLYTECHNIQUE
MONTREAL — QUEBEC — CANADA
JUNE 16-20, 1980

CONTROL DATA

INNOVATIVE NUMERICAL ANALYSIS FOR THE ENGINEERING SCIENCES

Proceedings of the Second International Symposium on Innovative Numerical Analysis in Applied Engineering Sciences

Edited by

R. Shaw

W. Pilkey

B. Pilkey

R. Wilson

A. Lakis

A. Chaudouet

C. Marino

University Press of Virginia
Charlottesville

PP. 13-22

THEORY OF MAGNETIC CIRCUITS FOR NONLINEAR MAGNETIC FIELDS IN ELECTROMAGNETIC DEVICES

Yoshifuru Saito
Department of Electrical Engineering
College of Engineering
Hosei University
Kajinocho Koganei, Tokyo 184, Japan

INTRODUCTION

A knowledge of the magnetic fields in electromagnetic devices is of the utmost importance to the designer. With the development of digital computers, the numerical methods are being extensively used to calculate the magnetic fields in electromagnetic devices. The numerical method can be classified into two main groups. One is the finite difference method, which replaces partial derivatives by divided differences; the other is the finite element method which is based on variational formulations (e.g., Refs.[1-4]). In addition to these methods, this chapter proposes the magnetic circuit method, which does not require the approximate description of a solution but permits great freedom with respect to the geometrical disposition and size of discrete elements [5,6]. The method described in this paper is deduced by applying the magnetic circuit theory to the small discretized elements; therefore, the boundary conditions which arise in magnetic field problems are automatically satisfied. Moreover, the theory of magnetic circuits is based on the discretization of physical quantities, so that the magnetic fluxes instead of magnetic potentials are directly evaluated.

To elucidate the effects of the eddy currents and the magnetic saturation in an iron core, this paper examines the magnetic fields of a simple saturable reactor as an example.

THEORY OF MAGNETIC CIRCUITS IN TWO-DIMENSIONAL FIELDS

When we consider the magnetic field region shown in Fig. 1(a), we can obtain the relation between magnetic field intensity $H_{\overline{abcda}}$ and current density $J_{i,j}$ as

$$\int_{\overline{abcda}} H\,dl = \int_{S_{i,j}} J_{i,j}\,n\,da \tag{1}$$

where dl denotes the infinitesimally small distance along the contour $\overline{abcda}$, and n is the unit normal vector on the infinitesimally small area da. Moreover, the subscripts i,j refer to the mesh point in Fig. 1(a). The magnetic field intensity H, magnetic flux density B, and magnetic flux ϕ are generally related by

$$H = \frac{B}{\mu} \tag{2}$$

$$B = \frac{\phi}{\Delta S} \tag{3}$$

where ΔS and μ denote respectively the surface area normal to the flux path and the permeability of the material.

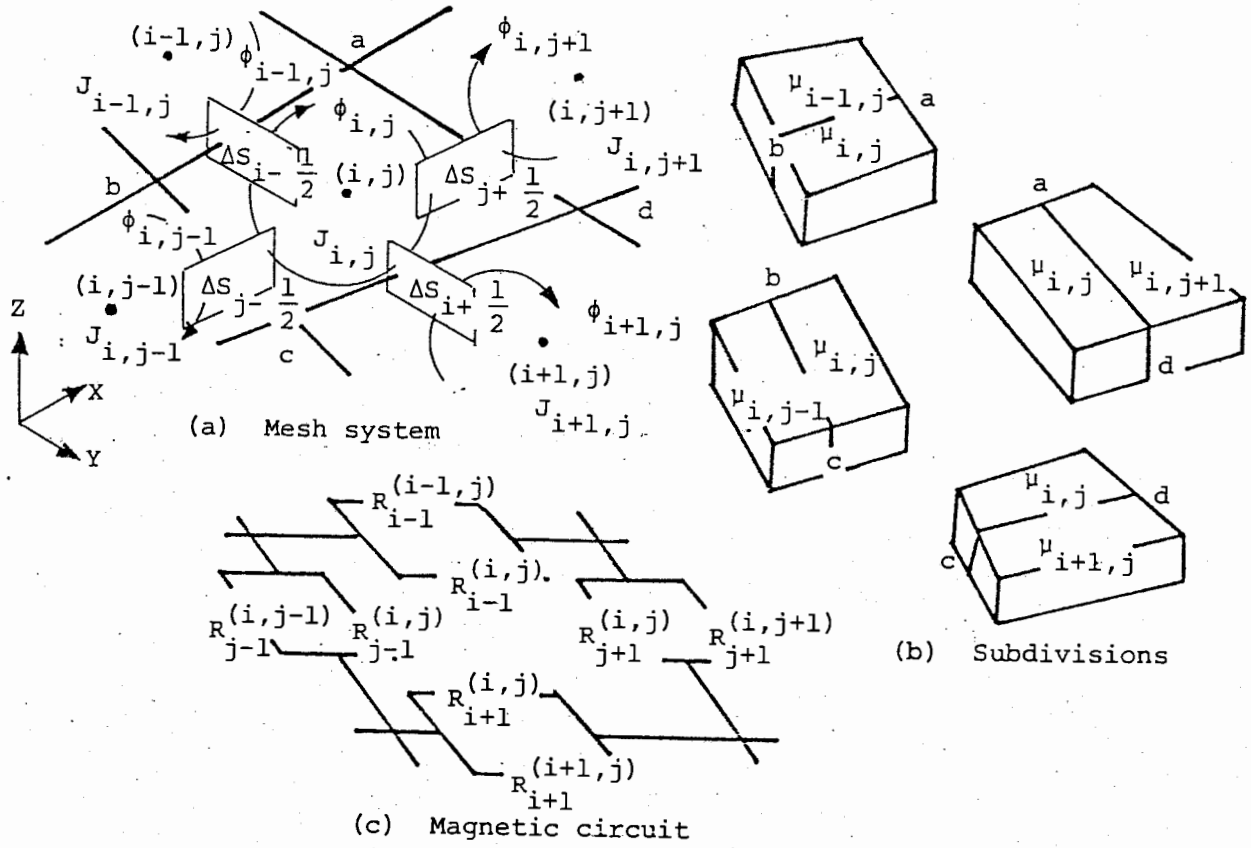

Fig. 1 Discretization of two-dimensional fields

Denoting the loop magnetic fluxes $\phi_{i,j}, \phi_{i\pm1,j}, \phi_{i,j\pm1}$ enclosing each of their mesh points in Fig. 1(a), by means of Eqs. (2) and (3), it is possible to write the left-hand term in Eq. (1) as

$$\int_{abcda} H dl = (\phi_{i,j} - \phi_{i-1,j}) \int_a^b \frac{dl}{\mu \Delta S_{i-(1/2)}} + (\phi_{i,j} - \phi_{i,j-1}) \int_b^c \frac{dl}{\mu \Delta S_{j-(1/2)}}$$

$$+ (\phi_{i,j} - \phi_{i+1,j}) \int_c^d \frac{dl}{\mu \Delta S_{i+(1/2)}} + (\phi_{i,j} - \phi_{i,j+1}) \int_d^a \frac{dl}{\mu \Delta S_{j+(1/2)}} \tag{4}$$

where $\Delta S_{i\pm(1/2)}, \Delta S_{j\pm(1/2)}$ denote the surface area normal to the loop magnetic fluxes. Equation (4) means that the magnetic field intensity $H_{\overline{abcda}}$ as well as magnetic flux densities around the mesh point (i,j) in Fig. 1(a) may take different values with respect to the positions but the magnetic flux which takes the paths along the contours $\overline{ab}, \overline{bc}, \overline{cd}, \overline{da}$ may take a constant value. In Eq. (4), the terms which depend on the geometrical shape as well as permeability of the material are known as the magnetic resistances. The magnetic resistance calculation with various geometrical shapes is described in detail

in Ref. [5]. Due to the nonlinear magnetization characteristic of iron, the permeability μ at each position takes a different value with respect to the position. Therefore, it is assumed that the region which encloses each of the mesh points in Fig. 1(a) may have a distinct value. Thereby, the magnetic fields in the region containing iron may be calculated as if this region is composed of different materials by the difference of permeability. At the interfaces of different materials, the tangential component of magnetic field intensity as well as the normal component of magnetic flux density must be continuous. In order to satisfy these boundary conditions, it is assumed that the magnetic resistances in Eq. (4) are calculated on the subdivisions shown in Fig. 1(b). This means that the current densities $J_{i,j}, J_{i\pm1,j}, J_{i,j\pm1}$ in Fig. 1(a) are not uniformly distributed on the surfaces $S_{i,j}, S_{i\pm1,j}, S_{i,j\pm1}$ but concentrated on the conductors with infinitesimally small cross-sectional areas located at each of their mesh points $(i,j),(i\pm1,j),(i,j\pm1)$, because it is difficult to calculate the magnetic resistance of the subdivision including the current density.

Under the dynamic condition, the current $I_{i,j}$, which is flowing on the conductor with infinitesimally small cross-sectional area located at the mesh point (i,j) in Fig. 1(a), is divided into two components: one is the eddy current due to the rate of change of magnetic flux $\phi_{i,j}$ in time t; the other is produced by the externally impressed voltage $E_{i,j}$, that is,

$$I_{i,j} = \int_{S_{i,j}} J_{i,j}\,nda = (1/r_{i,j})[E_{i,j} - (d/dt)\phi_{i,j}] \tag{5}$$

where d/dt denotes the time derivative, and $r_{i,j}$ is the electric resistance defined in the direction of z-axis in Fig. 1(a). The electric resistances with various geometrical shapes are calculated in much the same way as the magnetic resistance, since the definition of electric resistance with respect to the geometrical shape is similar to the definition of magnetic resistance. For further details, the reader should see Refs. [5-7]. When Eqs. (4) and (5) are substituted into Eq. (1), then we can formally obtain the magnetic circuit equation in dynamic state as

$$(\phi_{i,j}-\phi_{i+1,j})R_{i+(1/2)} + (\phi_{i,j}-\phi_{i,j-1})R_{j-(1/2)} + (\phi_{i,j}-\phi_{i-1,j})R_{i-(1/2)}$$

$$+(\phi_{i,j}-\phi_{i,j+1})R_{j+(1/2)} = (1/r_{i,j})[E_{i,j} - (d/dt)\phi_{i,j}] \tag{6}$$

where $R_{i\pm(1/2)}, R_{j\pm(1/2)}$ denote the magnetic resistances enclosing the mesh point (i,j) in Fig. 1(a). Each of these magnetic resistances is divided into two magnetic resistances by the difference of permeability (see Fig. 1(c)).

In the region containing iron, the permeability μ depends on the magnetic field intensity at each position, viz.,

$$\mu = f(H) \tag{7}$$

where f(H) denotes a function of H. With $V_{i,j}$ denoting the volume of the region taking the permeability $\mu_{i,j}$ in Fig. 1(b), the relationship between the magnetic field energy $P_{i,j}$ stored in the region taking the permeability $\mu_{i,j}$ and magnetic field intensity $H_{\overline{abcda}}$ along the contour line $\overline{abcda}$ in Fig. 1(a) is given by

$$P_{i,j} = (1/2)\mu_{i,j} H^2_{\overline{abcda}} V_{i,j} \tag{8}$$

The magnetic field energy P_m, magnetic resistance R_m, and magnetic flux ϕ are generally related by

$$P_m = (1/2)R_m\phi^2 \tag{9}$$

By means of Eqs. (7)-(9), it is possible to obtain the permeability $\mu_{i,j}$ as a function of the magnetic fluxes and of the permeabilities in Fig. 1(b).

THEORY OF MAGNETIC CIRCUITS IN THREE-DIMENSIONAL FIELDS

Most electromagnetic devices consist of conducting wires around an iron core. When the exciting current is flowing through the conducting wire, in order to minimize the magnetic field energy stored in the iron core, the eddy currents in the iron core flow in a direction opposite to the exciting current. The magnetic flux which passes through the path parallel to the current-carrying coil can be neglected; therefore, it is preferable to consider the solid element as shown in Fig. 2(a). The permeability of this solid element is determined from the magnetic field intensities in the radial and in the tangential directions. Also, the central portion of the solid element in Fig. 2(a) is one of the solid element; the permeability of this element becomes a function of magnetic field intensity in the tangential direction, because the magnetic resistance in the radial direction reaches infinitely large values.

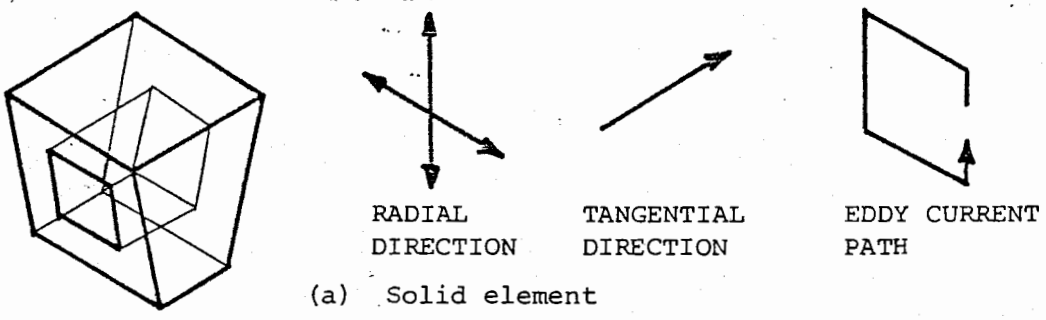

(a) Solid element

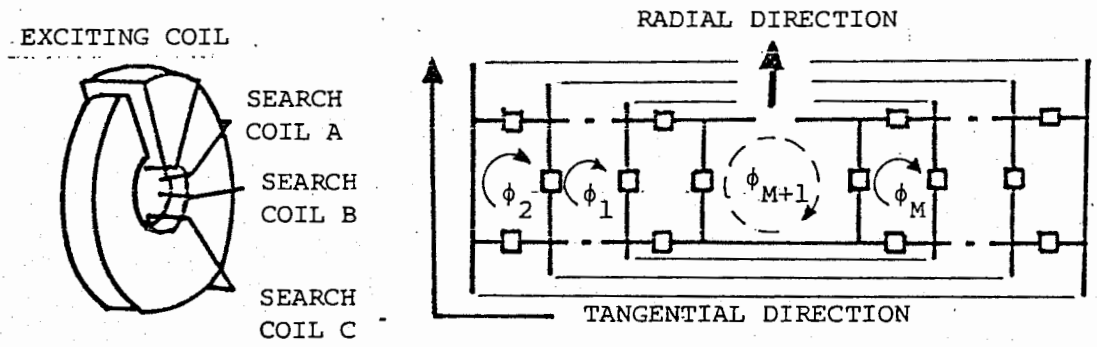

(b) Saturable reactor and its magnetic circuits

Fig. 2 Discretization of three-dimensional fields

For simplicity, it is preferable to consider a concrete example. One of the simplest examples of electromagnetic devices is the saturable reactor as shown in Fig. 2(b). This saturable reactor is divided into M_R parts in the radial direction and M_T parts in the tangential direction, taking into account the region containing air. Thereby, the magnetic field calculation of the saturable reactor is reduced to evaluate the $M(=M_R \times M_T)$ loop magnetic fluxes. Moreover, it is assumed that each of the exciting and search coils takes a distinct solid element which is similar in shape to the solid element shown in Fig. 2(a), and that no magnetic flux flows out of the boundary regions. The magnetic system of equations is preferably expressed in matrix notation involving the magnetic flux vector $\bar{\phi}$ (the notation $\bar{}$ refers to the vector quantities), externally impressed voltage vector $\bar{E}$, magnetic resistance matrix R, electric conductance matrix G, and winding matrix W. By introducing the relationship between the number of turns of coil and magnetic flux linkage into Eq. (6), the magnetic system of equations is expressed as

$$R\bar{\phi} = WG[\bar{E} - (d/dt)W\bar{\phi}] \tag{10}$$

For notational convenience, let the subscript (1) refer to the quantities related to the exciting coil; then the magnetic flux vector $\bar{\phi}$, which is a column matrix of order M, is written as

$$\bar{\phi} = [\phi_1, \phi_2, \ldots, \phi_M]^T \tag{11}$$

where superscript T refers to the transpose of the matrix. Also, the externally impressed voltage vector $\bar{E}$, electric conductance matrix G, and winding matrix W are respectively written as

$$E = [E_1, 0, \ldots, 0]^T \tag{12}$$

$$G = \text{diag.}\left[\frac{1}{r_1}, \frac{1}{r_2}, \ldots, \frac{1}{r_M}\right] \tag{13}$$

$$W = \text{diag.}[N_1, 1, \ldots, 1] \tag{14}$$

where r_1, r_2, r_M are respectively the electric resistances related to the loop magnetic fluxes ϕ_1, ϕ_2, ϕ_M. If one of the magnetic fluxes flows through the path containing air, the electrical resistance related to this magnetic flux will reach infinitely large values; N_1 denotes the number of turns of the exciting coil. The magnetic resistance matrix R in Eq. (10) is a square matrix of order M, viz.,

$$R = \begin{vmatrix} R_{11} & -R_{12} & \cdot & \cdot \\ & R_{22} & \cdot & \cdot \\ & & \cdot & \cdot \\ \text{SYMMETRICAL} & & & R_{MM} \end{vmatrix} \tag{15}$$

where the magnetic resistances $R_{11}, R_{12}, R_{22}, R_{MM}$ are easily obtained from the magnetic circuit in Fig. 2(b). By rearranging Eq. (10), it is possible to write Eq. (10) as

$$\bar{F} = Z\bar{\phi} \tag{16}$$

where F and Z are

$$\bar{F} = WG\bar{E}, \tag{17}$$

$$Z = (d/dt)WGW + R = (d/dt)L + R \tag{18}$$

When we compare the magnetic circuit in Fig. 2(b) with Eqs. (10)-(18), then it is found that the loop magnetic flux ϕ_{M+1} (shown by dotted line in Fig. 2(b)) must be taken into account in the calculation of magnetic fluxes to satisfy the condition of a minimum number of network equations [8]. Since the loop magnetic flux ϕ_{M+1} in Fig. 2(b) is physically flowing toward the tangential direction on the center of the radial direction, we can find the following relationship:

$$\bar{\phi} = C^T \bar{\phi}^C, \tag{19}$$

where $\bar{\phi}^C$ is the new transformed magnetic flux vector, C^T is the magnetic flux connection matrix, which is a rectangular matrix with M rows and (M+1)

columns, and superscript c refers to the transformed quantities. The magnetic flux connection matrix C^T is generally written as

$$C^T = \begin{vmatrix} 1 & 0 & 0 & . & -1 \\ 0 & 1 & 0 & . & -1 \\ . & . & . & . & . \\ . & . & . & . & -1 \end{vmatrix} \quad (20)$$

The transformation of a two-dimensional magnetic system of equations into a three-dimensional magnetic system of equations is carried out by

$$\overline{F}^c = Z^c \overline{\phi}^c \quad (21)$$

where $\overline{F}^c$ and Z^c are

$$\overline{F}^c = C\overline{F}, \quad (22)$$

$$Z^c = CZC^T = (d/dt)L^c + R^c \quad (23)$$

The details of the above transformation are described in Ref. [8-10].

The induced voltage vector $\overline{U}$ in electric circuits depends on the rate of change of magnetic flux in time t, that is,

$$\overline{U} = WC^T(d/dt)\overline{\phi}^c \quad (24)$$

Moreover, the current vector $\overline{I}$ is given in terms of the externally impressed voltage vector $\overline{E}$, induced voltage vector $\overline{U}$, and electric conductance matrix G, viz.,

$$\overline{I} = G(\overline{E} - \overline{U}) \quad (25)$$

By means of Eqs. (19)-(25), it is possible to obtain the magnetic fluxes, induced voltages, and currents in the saturable reactor.

NUMERICAL METHOD OF SOLUTION

With Δt denoting the step width, Eq. (21) is discretized in time by the following finite difference method:

$$[\alpha\overline{F}^c_{t+\Delta t} + (1-\alpha)\overline{F}^c_t] = (1/\Delta t)L^c[\overline{\phi}^c_{t+\Delta t} - \overline{\phi}^c_t] + [\alpha R_{t+\Delta t}\overline{\phi}^c_{t+\Delta t} + (1-\alpha)R_t\overline{\phi}^c_t], \quad (26)$$

where the parameter α can be chosen arbitrarily, e.g., $\alpha=0, \alpha=1/2, \alpha=1$ yield forward, central, and backward differences; subscript t and $t+\Delta t$ refer to the time t and $t+\Delta t$, respectively. The magnetic flux vector $\overline{\phi}^c_{t+\Delta t}$ in Eq. (26) is evaluated by the iteration method, using a relaxation parameter. The relaxation parameter ω is sequentially determined in every complete iteration. In order to determine the most suitable relaxation parameter, it is assumed that the relaxation parameter ω is equal to or greater than 1 but smaller than 2 and that the error of the solution taking the maximum absolute value is a function of the relaxation parameter, that is,

$$1 \leq \omega < 2 \quad (27)$$

$$\varepsilon = f(\omega) \quad (28)$$

where $f(\omega)$ and ε denote the function of ω and the error of the solution

taking maximum absolute value, respectively. Denoting $\omega^{(K)}$ the relaxation parameter used in K-th iteration, the relaxation parameter $\omega^{(K+1)}$ in the (K+1)th iteration is determined by the Newton Raphson method, viz.,

$$\omega^{(K+1)} = \omega^{(K)} - f[\omega^{(K)}]/[\partial f/\partial\omega]_{\omega = \omega^{(K)}} \tag{29}$$

However, it is difficult to calculate the term $\partial f/\partial\omega$ analytically. Therefore, this term is replaced by the backward difference:

$$[\partial f/\partial\omega]_{\omega = \omega^{(K)}} = [f(\omega^{(K)}) - f(\omega^{(K-1)})]/[\omega^{(K)} - \omega^{(K-1)}] \tag{30}$$

where $\omega^{(K-1)}$ is the relaxation parameter used in the (K-1)th iteration. By combining Eq. (29) with Eq. (30), it is possible to obtain the relaxation parameter $\omega^{(K+1)}$ in the (K+1)th iteration. If this relaxation parameter does not satisfy the condition of Eq. (27), then the relaxation parameter $\omega^{(K+1)}$ is reduced to satisfy this condition. Moreover, the relaxation parameters for the first and second iterations are respectively selected to be 1.5 and 1.6 in the calculation in this chapter. As shown in Fig. 3, the magnetic fluxes are overrelaxed, but the permeabilities are underrelaxed to suppress the variation of the elements in the magnetic resistance matrix $R^{c}_{t+\Delta t}$ in Eq. (26) [5,6]. Figure 3 shows the flow chart for this iteration method.

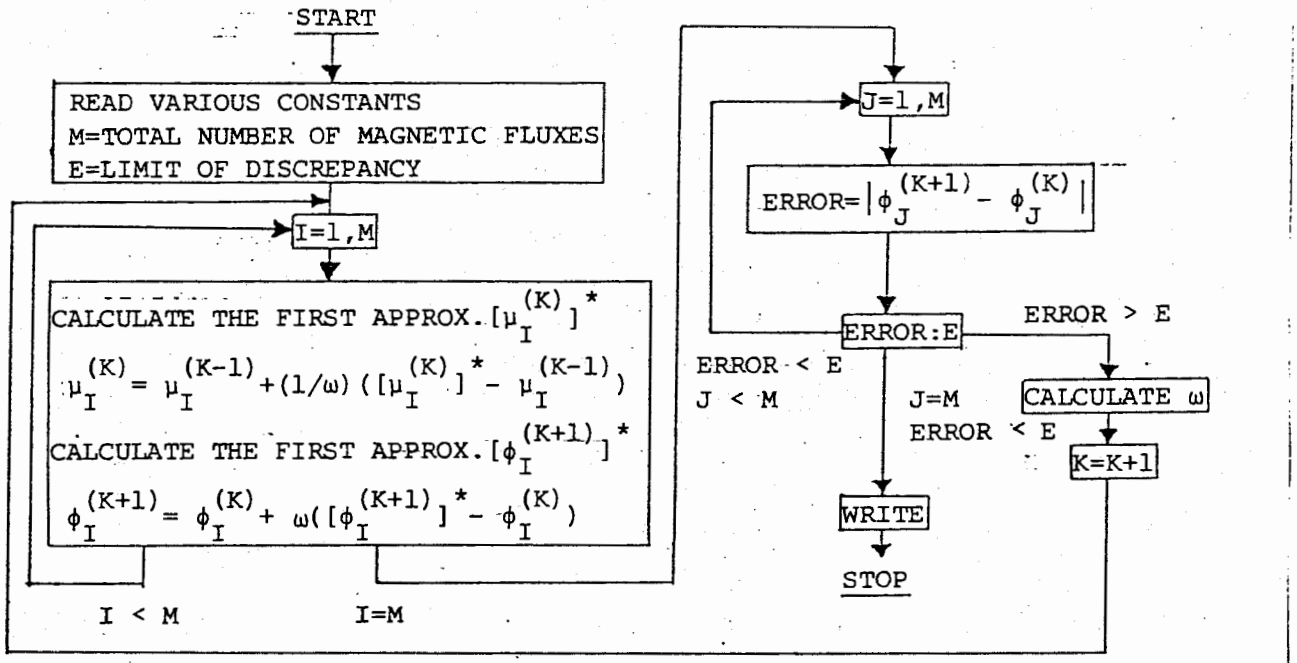

Fig. 3 Flow chart of the iteration method

By means of the central difference method, the induced voltage vector $\overline{U}$ of Eq. (24) and the current vector $\overline{I}$ of Eq. (25) are respectively given by

$$\overline{U}_{t+(\Delta t/2)} = \overline{WC}^{T}(1/\Delta t)(\overline{\phi}^{c}_{t+\Delta t} - \overline{\phi}^{c}_{t}) \tag{31}$$

$$\bar{I}_{t+(\Delta t/2)} = G(\bar{E}_{t+(\Delta t/2)} - \bar{U}_{t+(\Delta t/2)}) \tag{32}$$

where the subscript $t+(\Delta t/2)$ refers to the time $t+(\Delta t/2)$.

NUMERICAL EXAMINATION

Various constants used in the calculation of the saturable reactor shown in Fig. 2(b) are listed in Table 1. In carrying out the magnetic field calculation of the saturable reactor, the nonlinear magnetization characteristic of iron is introduced by linear interpolation [11].

Table 1 Various Constants Used in the Calculation

Number of subdivisions in the radial direction	8
Number of subdivisions in the tangential direction	12
Limit of discrepancy	0.0001 percent
Inner radius of iron core	0.025 [m]
Outer radius of iron core	0.035 [m]
Thickness of iron core	0.010 [m]
Thickness of exciting coil	0.003 [m]
Thickness of the region containing air	0.017 [m]
Number of turns of exciting coil	100 turns
Number of turns of search coil	25 turns
Electric resistance of exciting coil	1.21 [Ω]
Conductivity of iron core	1/80 [1/μΩcm]
Externally impressed voltage (step voltage)	5.0 [V]
Step width Δt	0.0001[sec]
All the initial magnetic fluxes and currents are set equal to zero.	

For comparison, the transient magnetic fluxes were calculated by the forward difference (α=0), central difference (α=1/2), and backward difference (α=1) methods. Among the results obtained by each method, the numerical solutions computed by the backward difference method were somewhat small compared with the results obtained by the central difference method. Likewise, the forward difference method produced such unstable solutions that this method became useless. Therefore, in this chapter, the magnetic field calculation of the saturable reactor was carried out by using the central difference method. The numerical tests using various step widths were carried out and it was found that the solutions using the step width Δt=0.0001 (sec) had satisfactory accuracy. In order to perform a good switching operation, a simple electronic switching circuit utilizing a silicon-controlled rectifier was used. Moreover, accuracy of the input step voltage wave form was confirmed. The numerical calculation was continued until the numerical solutions reached the steady state values. Figure 4(a) shows the relationship between steady state exciting currents and magnetic fluxes together with the experimental values. The numerical calculations were carried out under six different-step voltages so that the results shown in Fig. 4(a) were obtained. The experimental values in Fig. 4(a) were obtained by integrating the induced voltages at the search coils by an electronic integrator [12]. The transient exciting current and induced voltages at the search coils are shown in Fig. 4(b), together with the experimental values. When one considers the results of Fig. 4(b), it is obvious that the magnetodynamic fields in the saturable reactor are dominated considerably by the eddy currents flowing through the iron core.

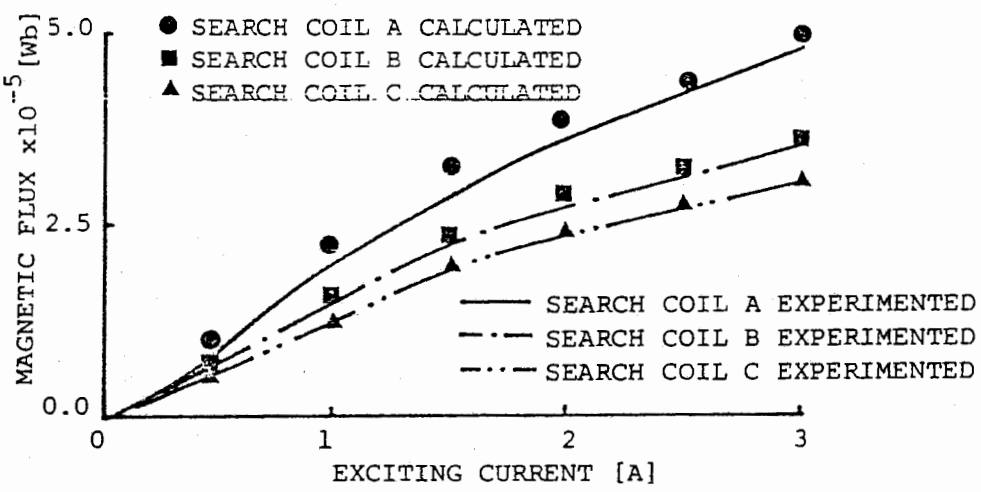

(a) Steady state

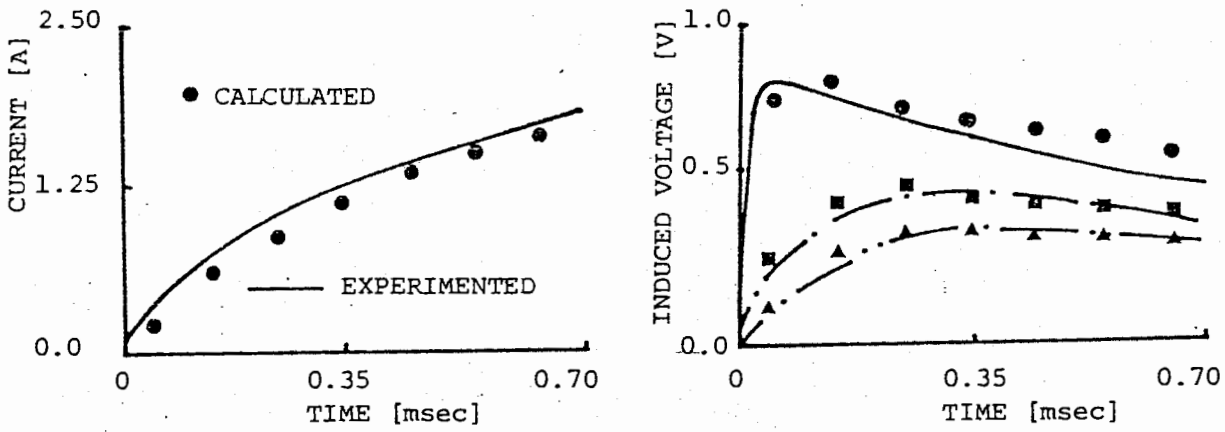

(b) Dynamic state (the notations of right-hand figre are the same as those the top figure.)

Fig. 4 Comparison of the experimental results with calculated results

CONCLUSION

As shown above, this chapter has shown that the theory of magnetic circuits is quite effectively applicable to the magnetic field problems in electromagnetic devices. The influences of the magnetic saturation and eddy currents in the saturable reactor have been clarified by the method of magnetic circuits as an example. Moreover, it has been shown that the system of magnetic circuit equations is effectively solved by the central difference method along with the iteration method. The operation count required to obtain the results of Fig. 4(b) was about 10 minutes on the computer FACOM 230-45S.

ACKNOWLEDGMENTS

The author is grateful to Professor I. Fujita and Professor T. Yamamura for their helpful advice and to Professor T. Nishiya and Mr. M. Kadoi for the facilities they provided at the Computer Center of Hosei University.

REFERENCES

1 Erdelyi, E.A., Ahamed, S.V., and Hopkins, R.E., "Nonlinear Theory of Synchronous Machines on Load," IEEE Trans. Power Apparatus and Systems, Vol. PAS-85, 1966, pp. 792-801.

2 Erdelyi, E.A., and Fuch, E.F., "Fields in Electrical Devices Containing Soft Nonlinear Magnetic Materials," IEEE Trans. Magnetics, Vol. MAG-10, 1974, pp. 1103-1108.

3 Silvester, P., and Chari, M.V.K., "Finite Element Solution of Saturable Magnetic Field Problems," IEEE Trans. Power Apparatus and Systems, Vol. PAS-89, 1970, pp. 1642-1651.

4 Chari, M.V.K., and Silvester, P., "Finite Element Analysis of Magnetically Saturated DC Machines," IEEE Trans. Power Apparatus and Systems, Vol. PAS-90. 1971, pp. 2362-2372.

5 Saito, Y., "Three-Dimensional Analysis of Nonlinear Magnetostatic Fields in a Satirable Reactor," Comp. Meths. Appl. Mech. Eng., Vol. 16, No. 1, Oct. 1978, pp. 101-115.

6 Saito, Y., "Method of Magnetic Circuits for Nonlinear Magnetostatic Fields in Polyphase Induction Motors at No-Loads," Comp. Meths. Appl. Mech. Eng., Vol. 13, No. 1, January 1978, pp. 105-118.

7 Stratton, J.A., Electromagnetic Theory, McGraw-Hill, New York, 1941, pp. 13-16.

8 Messerle, H.K., Dynamic Circuit Theory, Pergamon, Oxford, 1965, pp. 117-167.

9 Guillemin, E.A., The Mathematics of Circuit Analysis, M.I.T. Press, Cambridge, Mass., 1969, pp. 135-137.

10 Hancock, N.N., Matrix Analysis of Electrical Machinery, Pergamon, Oxford, 1974, pp. 24-36.

11 Trutt, F.C., Erdelyi, E.A., and Hopkins, R.E., "Representation of the Magnetization Characteristic of DC Machines for Computer Use," IEEE Trans. Power Apparatus and Systems, Vol. PAS-87, 1968, pp. 665-669.

12 Scott, N.R., Electronic Computer Technology, MacGraw-Hill, New York, 1970, pp. 9-11.